Proceedings of GT2005
ASME Turbo Expo 2005: Power for Land, Sea, and Air
June 6-9, 2005, Reno-Tahoe, Nevada, USA

GT2005-68479

HIGH PRESSURE TURBINE DEPOSITION IN LAND BASED GAS TURBINES FROM VARIOUS SYNFUELS

Jeffrey P. Bons, Jared Crosby, James E. Wammack, Brook I. Bentley
Department of Mechanical Engineering, Brigham Young University, Provo, UT 84602

Thomas H. Fletcher
Department of Chemical Engineering, Brigham Young University, Provo, UT 84602

ABSTRACT

Ash deposits from four candidate power turbine synfuels were studied in an accelerated deposition test facility. The facility matches the gas temperature and velocity of modern first stage high pressure turbine vanes. A natural-gas combustor was seeded with finely-ground fuel ash particulate from four different fuels: straw, sawdust, coal, and petroleum coke. The entrained ash particles were accelerated to a combustor exit flow Mach number of 0.31 before impinging on a thermal barrier coating (TBC) target coupon at 1150°C. Post exposure analyses included surface topography, scanning electron microscopy, and x-ray spectroscopy. Due to significant differences in the chemical composition of the various fuel ash samples, deposit thickness and structure vary considerably for each fuel. Biomass products (e.g. sawdust and straw) are significantly less prone to deposition than coal and petcoke for the same particle loading conditions. In a test simulating one turbine operating year at a moderate particulate loading of 0.02 parts per million by weight, deposit thickness from coal and petcoke ash exceeded 1 mm and 2 mm respectively. These large deposits from coal and petcoke were found to detach readily from the turbine material with thermal cycling and handling. The smaller biomass deposit samples showed greater tenacity in adhering to the TBC surface. In all cases, corrosive elements (e.g. Na, K, V, Cl, S) were found to penetrate the TBC layer during the accelerated deposition test. Implications for the power generation goal of fuel flexibility are discussed. [*Keywords:* deposition, syngas, turbines]

NOMENCLATURE

ESEM environmental scanning electron microscope
TBC thermal barrier coating

INTRODUCTION

Due to current economic and political pressures, alternate fuels such as coal, petcoke, and biomass are being considered to produce substitute syngas fuels to replace natural gas in power turbines. Given the present volatility in natural gas markets and the uncertainty regarding projected fuel availability over the 20-30 year design lifetime of newly commissioned power plants, coal and petroleum derivative fuels are already being used at a handful of gas turbine power plants worldwide. In addition, intermediate goals of the DOE Future Gen and DOE Turbine Program focus on coal syngas as a turbine fuel in an effort to reduce dependency on foreign supplies of natural gas. At the same time, environmental concerns have led to government mandated biomass utilization in boilers in some European countries. Biomass turbine power plants are of particular interest since they would potentially provide a CO_2 emission benefit without expensive CO_2 capture and sequestration. Thus, the stage is set for broader integration of alternate fuels in gas turbine power plants.

Despite the greatest precaution in filtration and cleanup systems, small levels of unwanted contaminants are introduced into the hot section of gas turbines. At the high mass flow rates typical of large utility engines, even trace amounts of particulate can accumulate to significant quantities. For example, a particulate concentration of 0.1 parts per million by weight (ppmw) will produce 2 tons of ingested material in a large utility power plant during an 8000 hour operating year. These contaminants may either pass through the engine with no effect, or attack the surfaces of the engine through erosion, corrosion, or deposition. The adverse effects of these three degradation mechanisms are well documented in the literature. Erosion reduces engine performance by opening up tip clearances and altering blade contours. For example, Ghenaiet et al. [1] reported a 6-10% loss in adiabatic efficiency for 6 hours of sand ingestion in an axial fan. Deposition poses the opposite problem by clogging critical bleeds and reducing blade flow passages. Wenglarz [2] proposed a model for estimating the loss in turbine power that occurs when the choked mass flow limit is reduced due to deposit buildup at the

nozzle guide vane passage throat. Kim et al. [3] documented the disastrous results of film cooling holes being plugged by massive ingestion from simulated volcanic ash in aircraft gas turbines. Deposition can also accelerate material corrosion by bringing significant concentrations of corrosive elements in direct (molten) contact with the turbine material system. Both erosion and deposition are also known to increase levels of surface roughness, which produces corresponding increases in heat transfer (up to 50%) and skin friction (up to 300%) [4]. Finally, all three degradation mechanisms (including corrosion) reduce part life and increase the risk of run-time failure.

The prevailing mode of surface degradation for a given combination of airborne contaminants is a function of the specific turbine operating environment. Two of the important determining factors are the gas (and particle) temperature and the turbine surface temperature. The gas temperature determines the physical state of the particles (e.g. solid, molten, or vapor). This in turn influences whether the particles rebound from the surface (potentially causing erosion upon impact) or instead tend to deposit. Previous turbine tests with coal-derived fuels by Wenglarz and Fox [5,6] show a dramatic increase in deposition rate as the gas temperature is raised above the particulate melting point. In their study, coated turbine superalloy specimens were subjected to 2-5 hours of deposition from three coal-water fuel (CWF) formulations. The coal had been cleaned to simulate ash levels (~1%) that would be considered acceptable for use in a gas turbine. The ash consisted primarily of Fe, Si, Al, and Ca with <2% concentrations of K, Na, P, Ti, and Mn. The fuel was burned in a low-emission subscale turbine combustor at realistic flow rates (e.g. impact velocities ~ 180m/s) and gas temperatures (1100°C). With the turbine specimens located at two different streamwise locations downstream of the combustor exit, the influence of gas temperature on deposition rate could be studied. It was noted that the upstream specimens (operating at gas temperatures ~ 1100°C) experienced 1 to 2 orders of magnitude higher deposition rates compared to the downstream specimens (operating at gas temperatures ~ 980°C). High temperature deposits were primarily Fe, Al, and Si while the lower temperature deposits had a disproportionately high concentration of Na. This corresponded with the lower softening temperature of Na compared to Al and Si. Also, the lower temperature deposit spalled off with test shutdown while the higher temperature deposits adhered to the surface more tenaciously. Compared to a previous series of tests with lower ash content (0.025%) residual fuel oil, the deposit levels with coal-water fuels were 2 to 3 orders of magnitude larger for the same operating temperature [7].

Wenglarz and Fox [5] also explored the possibility of sub-cooling the upstream turbine specimens and found a factor of 2.5 reduction in deposits for a 200°C drop in metal surface temperature. Lower deposit formation in areas of reduced surface temperature was also noted by Bons et al. [8] in their study of serviced turbine hardware. Cooled turbine vanes which exhibited large (1-2 mm thick) marine deposits over their entire surface were noticeably free of deposits in the film cooling flow path where surface temperatures are significantly lower. This effect created substantial troughs or "furrows" which extended for more than 10 hole diameters downstream of the cooling hole exit. These results confirm the important role of gas and surface temperature in determining deposition rates from ash-bearing fuels.

For biomass fuels, Patnaik et al. [9] conducted flame tunnel tests on MCrAlY (oxidation resistant coating) and TBC (thermal barrier coating) material systems using a wood pulp liquid fuel suspension. Specimen temperatures of 850°C and 650°C were attained to simulate conditions in a gas turbine, though gas velocities were not representative. The study focused on the corrosive influence of alkali elements in the high-ash content biomass fuel. These elements can not be washed out with standard scrubbing techniques. Ash deposits of up to 2 mm in thickness were observed after 50 hours of exposure to the high temperature biomass flame. The actual deposition rate may have been significantly larger than this given evidence of deposit flaking and renewal during the test duration. The deposits consisted primarily of K and Ca, with smaller concentrations of Ni, Si, Cu, Cr, and S. Subsequent 1000 hr corrosion tests at constant temperature yielded evidence of Type I hot corrosion despite low levels of sulfur present in the deposit. Significant coating degradation and removal was noted due to repeated fusing and flaking off of deposits during the flame exposure test.

In a related study, Wright et al. [10] reviewed the composition of typical biomass fuels (grass-based and wood-based) and assessed the relative degradation threat posed to gas turbines by these renewable fuels compared to coal. Wood and grass-based biomass fuels both have higher levels of corrosive alkali metals such as K and Na than coal. Of the two classifications studied, grass-based fuels were identified as having the potential to be most troublesome due to higher levels of S and Cl. Similar to Patnaik et al. [9], this study by Wright et al. concluded that biomass cleanup to remove alkali is more problematic than coal due to the high moisture content.

Considering these well-documented findings, power plant operators and manufacturers interested in promoting fuel flexibility in gas turbines would do well to consider issues related to deposition from higher ash content fuels. This is particularly critical in light of recent advances in turbine material systems which now routinely allow turbine inlet temperatures in excess of 1400°C. At these elevated temperatures, more stages of a gas turbine encounter gas (and particles) at temperatures in excess of particle melting temperature, and are thus more susceptible to deposition. Moreover, modern G and H-class turbines rely heavily on innovative cooling strategies which may influence deposition patterns in the flow path. Finally, advanced material systems (EB-PVD and APS TBCs) have been designed and validated during a period when natural gas is the gas turbine fuel of choice. As such, the impact of depositing contaminants on TBCs may present unforeseen viability issues for existing high-performance turbines. Clearly, new research is needed to evaluate the impact of alternate fuels in this complex operating environment.

The objective of the present study is to provide a comparative analysis of various fuel alternatives at engine representative conditions. This is done using the recently commissioned Turbine Accelerated Deposition Facility (TADF) described in detail by Jensen et al. [11]. The design premise of this test facility is that deposition in gas turbines is governed by essentially three critical parameters: gas (particle) temperature, gas (particle) impact velocity, and particle

loading. Gas temperature insures that the particles are in the correct physical state (solid, molten liquid, or vapor) when they arrive at the turbine surface, particle velocity governs the primary delivery mode of inertial impaction, and particle loading is the net particle loading experienced by the turbine over a given period of time. The latter of these three simulation parameters is potentially the most controversial since it implies that 4,000 hours of deposition exposure on a real gas turbine can be simulated with a 4 hr accelerated laboratory test as long as the net particle throughput is matched. Thus, by increasing the particle concentration in the combustor gas (parts per million by weight, or ppmw) by three orders of magnitude from that found in a typical operating turbine, the test duration can be reduced by the same three orders of magnitude to preserve the same particle loading [ppmw-hr]. The validation of this hypothesis was the subject of a previous paper by Jensen et al. [11]. Heat transfer characteristics of deposits generated in the accelerated deposition facility were compared with deposits on in-service hardware. It was found that for all of the critical features affecting convective heat transfer (i.e. deposit surface roughness) and conduction heat transfer (i.e. deposit thickness, structure, and elemental constituents), the accelerated test produced comparable results to longer duration exposure.

Using this accelerated facility, the influence of different operating parameters on deposition can be rapidly evaluated in a comprehensive test matrix. For example, a previous study considered the effect of gas temperature and impingement angle on deposit formation from airborne particles typical of dust-laden operating environments [11]. The present study addresses the effect of different fuels at constant operating conditions.

ASH PREPARATION AND CHARACTERIZATION

To avoid the considerable capital expense and complexity associated with simulating combustor operation with different fuel formulations (e.g. fluidized bed, gas cleanup system, etc.), the Turbine Accelerated Deposition Facility (TADF) employs a natural gas combustor seeded with ash particles. Thus, it is critical to insure that the ash particles are of the same size, state, and composition that might be expected to impact on turbine surfaces after reasonable gas cleanup.

The four ash samples used in this study were collected from various sources. Coal and petcoke samples were obtained externally, while the biomass samples were prepared locally using facilities in BYU's Advanced Combustion Engineering Research Center (ACERC). Subbituminous coal fly ash was obtained from an operating power plant, while the petcoke ash is boiler slag obtained from a combined cycle gas turbine power plant operating with a blend of 55% petcoke and 45% coal. Straw ash was produced in a two-step process. First, raw material was partially burned to eliminate volatiles. Second, the partially burned ash was placed in a programmable furnace and cycled through a standard ashing process. This same two step process was repeated to generate sawdust ash. A standard kitchen wheat grinder set on the finest setting was used to grind the ash particles to the size needed for testing.

Since the objective of the study was to simulate ash that could be entrained by the flow leading to the turbine, the particles must be small enough to navigate the various gas cleanup systems. Filtration systems in modern gas turbine powerplants are designed to remove all particles with diameters greater than 10 μm and a majority of particles larger than 1 μm. Measurements of particle size distributions from properly functioning advanced filtration systems indicate mass mean diameters (MMD) of order 1 μm, even for hot gas clean-up. With inadequate or degraded filtration, these levels can be exceeded. Thus the target mass mean particle diameter for this study was less than 10 μm. After grinding, the size of each ash sample was determined using a laser-based Coulter Counter. The ash was suspended in distilled water and dispersed through the Coulter Counter feed system with the use of a sonicator and/or small amounts of liquid detergent. When illuminated by the laser beam, the particles scatter light in patterns according to their size. This scattered light was detected using photodetectors and converted to the particle distributions shown in Figure 1; mass mean diameters are presented in Table 1. With the exception of the petcoke sample, the mass mean diameters are all between 10-20 μm, with a significant portion of each sample under 10 μm. Thus, the majority of particles in this study are larger than those found with properly functioning gas cleanup. Larger particles (>1 μm) are deposited by inertial impaction while smaller particles (<1 μm) are generally deposited by turbulent diffusion and thermophoresis. Thus, the results of this study are appropriate for deposition dominated by inertial impaction. Nearly all of the particles are less than 40 μm in diameter, which was determined to be the maximum diameter that would attain full velocity and thermal equilibrium with the hot gases in the combustor exit nozzle of the TADF [11]. Thus, the particles are expected to be at the proper gas temperature before impact.

Table 1: Ash particle summary statistics: size, density, and elemental composition.

	Coal	Petcoke	Straw	Sawdust
Mass mean diameter (μm)	13.3	33.0	17.6	19.7
Median diameter (μm)	10.6	28.5	15.1	11.8
Bulk density (g/cc)	0.99	1.45	0.84	0.48
Apparent density (g/cc)	1.98	2.90	1.68	0.96
Elements in order of atomic number	Weight %	Weight %	Weight %	Weight %
Na	6.9	4.3	1.7	5.9
Mg	3.6	2.2	2.54	12.4
Al	17.8	14.5	1.8	5.1
Si	47.4	38.3	48.4	11.6
P	1.6	0.0	3.4	2.2
S	1.8	1.0	3.0	1.3
Cl	0.0	0.0	2.8	0.0
K	2.6	2.5	23.4	10.7
Ca	8.7	7.5	7.8	42.9
Ti	1.6	0.8	0.0	1.3
V	0.0	3.4	0.0	0.0
Cr	0.0	0.0	0.0	0.0
Mn	0.0	0.0	0.0	4.5
Fe	6.4	22.9	5.0	1.0
Ni	0.0	0.9	0.0	0.0

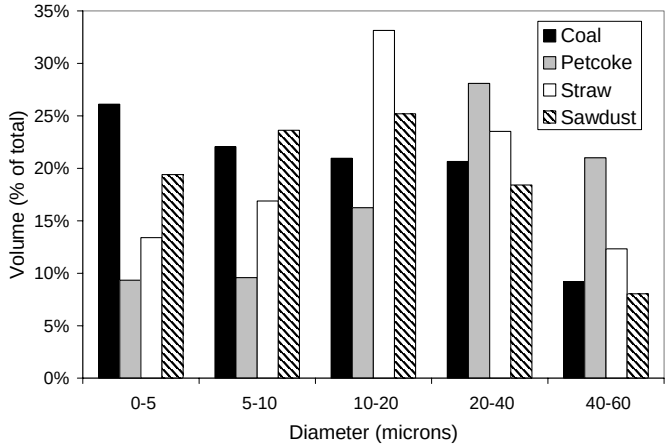

Figure 1: Ash particle size distribution from Coulter Counter measurement.

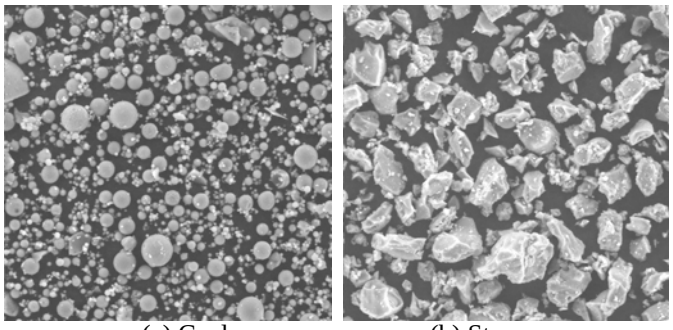

(a) Coal (b) Straw

Figure 2: ESEM images of (a) coal and (b) straw ash after processing. Images are approximately 150μm x 150μm.

Following the Coulter Counter measurement, ash samples were placed inside a FEIXL30 environmental scanning electron microscope (ESEM) to obtain qualitative validation of the particle size and shape. Figure 2 show typical ESEM images from two of the ash samples. The coal ash particles appeared mostly spherical in shape while the straw ash particles were more uniform in size but more irregular in shape. The petcoke ash (not shown) was similar to the straw in shape though not in size. Finally, the sawdust ash particles (not shown) were highly irregular with indistinct boundaries between clumps and edges that appeared fibrous. The bulk density of each ash sample was measured in a graduated cylinder, and the apparent density (mass per particle exterior volume) was calculated using an estimated packing factor of 0.5 (see Table 1).

X-ray spectroscopy was used to determine the composition of the four types of ash while they were in the ESEM. An EDAX Phoenix Spectrometer with super ultra-thin window was used to obtain elements down to an atomic number of carbon. The elemental compositions of the four types of ash, as determined by the x-ray analysis, are given in Table 1. Values of 0.0 indicate levels below the background noise level of the spectrometer. An independent elemental analysis was conducted on the four ash samples by ALS Chemex using inductively coupled plasma atomic emission spectroscopy (ICP-AES). The results identified the same elements as the x-ray spectrometer in approximately the same weight percentages, though the ICP-AES analysis of the bulk ash showed 15-20% greater silicon content compared to the x-ray measurements which were spot measurements. Also, the ICP-AES is unable to measure vanadium.

Of particular note in Table 1 are the high levels of S and Cl in straw (as noted by Wright et al. [10]) and the vanadium found in petcoke (added during petroleum processing). Petcoke also shows particularly high levels of iron-oxide. Calcium and magnesium are especially prevalent in the sawdust ash while sodium is indicated in all of the samples, though at a lower level in straw ash. The potassium levels in biomass are also significantly higher than coal and petcoke, as noted earlier.

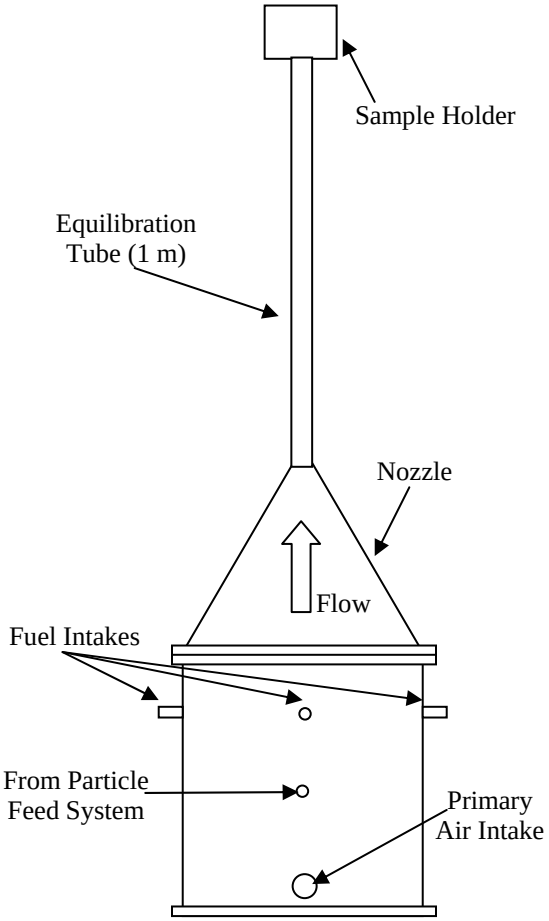

Figure 3: Schematic of Turbine Accelerated Deposition Facility (TADF) at BYU

EXPERIMENTAL TEST CONDITIONS

A detailed description of the Turbine Accelerated Deposition Facility (Figure 3) is provided by Jensen et al. [11]; only a brief summary of the essential features is given here. High pressure air is fed into the base of the combustor, where it is properly dispersed and straightened to provide uniform flow to the burner with no swirl. Natural gas is fed into the combustor through four symmetrically-placed copper tubes. A small amount of air is premixed with the natural gas. This partial premixing drastically reduces soot formation in the facility, but for safety considerations the amount of air added is kept small to avoid the flammability limit. A fraction of the high pressure air is also directed through the particle feed system where the ash particulate is injected into the center of

the combustor. The particle feed system consists of a glass bulb that has two inlets and one exit. The primary air enters through the top and the particulate is steadily injected through a side inlet by a glass syringe driven by an electric motor. The particulate-carrying flow exits from the bottom of the bulb to the combustor. Test conditions are monitored using mass flow and temperature sensors. Air flow is measured by a choked flow orifice plate. The natural gas mass flow rate is determined using a rotameter and a pressure gauge in the line. The uncertainty in the mass flow was ±4% for the nominal flow rate (0.011 kg/s).

After combustion the flow enters a 20° cone axisymmetric nozzle with a 370:1 inlet to exit area ratio. This is followed by a 1 m long pipe where entrained particles less than 40 μm in size reach 95% of the flow velocity and temperature before impacting the test specimen. The flow exits this equilibration pipe as a turbulent jet and impinges on the target coupon located 2-3 jet diameters from the pipe exit (Figure 3). Jet exit temperatures were measured using two Super OMEGACLAD K-type thermocouple probes positioned just upstream of the turbine blade sample. Overall error in temperature measurements is less than 15°C at the operating temperature of 1150°C.

Table 2: Particle loading test conditions.

Ash Type	Test Duration [hrs]	Particle concentration [ppmw]	Net particle loading [ppmw-hr]	Net deposit weight [mg]	Deposition rate [mg/cm^2 hr]	Net particle capture efficiency [%]
Coal	3	55	165	1.1	72	17%
Petcoke	2	70	140	Not measured	N/A	N/A
Straw	2	77	154	<0.1	N/A	N/A
Sawdust	3	37	111	0.2	13	5%
Coal	4	150	600	2.9	143	12%
Petcoke	3	165	495	1.15	76	6%

Particle feeding commenced after the facility was brought to steady-state operating conditions, which were maintained throughout the duration of each test. The steady-state conditions at the combustor exit were approximately 1150°C with a 200 m/s exit velocity (Mach number of 0.31), matching the typical inlet Mach number range (0.2-0.4) for a first-stage turbine blade row. As mentioned earlier, the operating principle of the accelerated deposition facility is to match the net loading of particulate, measured in ppmw-hrs. Table 2 contains the test duration and ppmw-hrs loading data. The majority of testing was conducted at a nominal value of 140 ppmw-hrs, while two additional tests were performed at significantly higher loadings. As a reference, the 140 ppmw-hr loading level would be equivalent to 1 operating year (8,000 hrs) at a relatively low particulate concentration of 0.02 ppmw.

Circular turbine blade samples, approximately 2.41 cm in diameter and 0.45 cm thick, were obtained from a turbine blade coating manufacturer. The samples were representative of a high performance turbine material system: a cobalt based super alloy substrate approximately 0.3 cm thick, an MCrAlY oxidation resistant coating approximately 125 μm thick, and an air plasma sprayed (APS) yttrium stabilized zirconium (YSZ) thermal barrier coating (TBC) layer approximately 0.75 mm thick. All tests were run with the samples at a 45 degree impingement angle. No cooling was applied to the specimen, so the system operates approximately isothermally at the gas temperature. Temperature gradients through the TBC thickness that exist in practice are therefore not simulated.

After completing the tests each sample was weighed and compared to its pre-burn weight. The samples were then placed on a Hommel profilometer to measure the surface topography and roughness of the deposits. Multiple steps were required to prepare the sample for analysis in the ESEM. Each sample was potted in epoxy to preserve the deposit. Using a water-cooled, diamond tipped saw, each sample was cut in half perpendicular to the flow direction. The cut sample was then encased in bakelite and polished. Finally, because deposit layers and TBC are not electrically conductive, the sample was coated with a fine layer of carbon to prevent charge buildup from distorting the ESEM images.

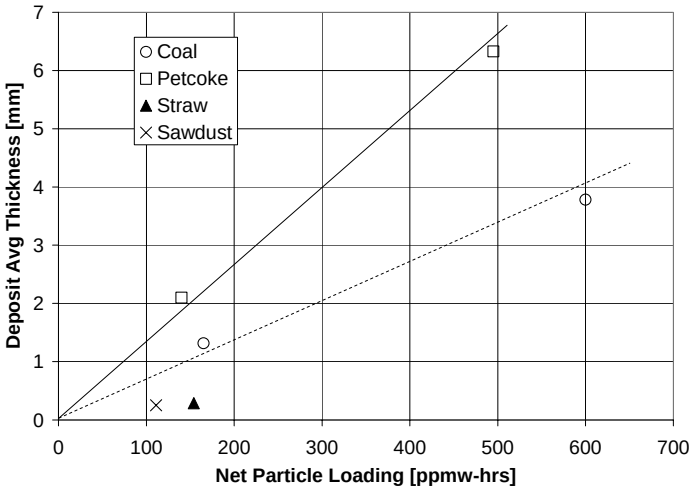

Figure 4: Average deposit thickness vs. net particle loading for 4 fuels.

RESULTS AND DISCUSSION

After cross-sectioning each specimen, the average deposit thickness was determined from a series of point measurements made every 3 mm along the cut section. This average thickness data are plotted vs. net particle loading (ppmw-hrs) in Figure 4. Since the cross-section was deliberately taken through the peak thickness of the deposit, this measurement is a linear average and does not represent an average for the entire specimen surface area. From the limited coal and petcoke data it appears that the deposit thickness varies linearly with net particle loading (as denoted by the lines from the origin).

Using the pre-test and post-test weight measurements, the net specimen weight gain during exposure was assessed (Table 2). Dividing this deposit weight by the exposed coupon surface area and the test duration yielded deposition rate measurements of 143 mg/cm^{2}hr and 76 mg/cm^{2}hr for the highest particle loading coal and petcoke cases, respectively (Table 2). This coal deposition rate is comparable to those witnessed in the coal water fuel study of Wenglarz and Fox [5] where deposition rates from 200-400 mg/cm^{2}hr were recorded at comparable gas temperatures. The petcoke deposit is a factor of 4 less dense than the coal deposit. It has twice the average thickness but only half the weight. This is indicative of the porous nature of

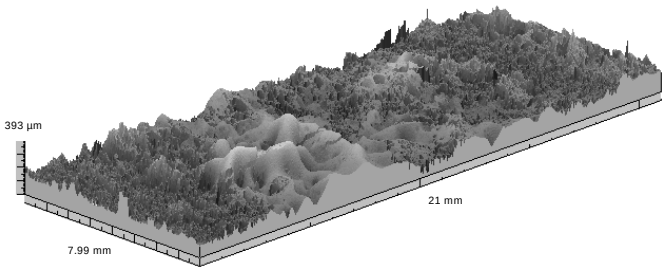

a) 8mm x 21mm section of straw deposit surface – peak height ~400µm

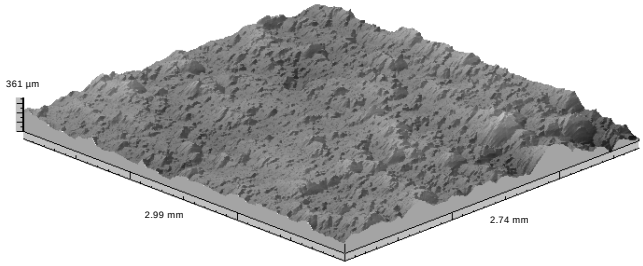

b) 3mm x 3mm section of coal deposit surface – peak elevation ~600µm

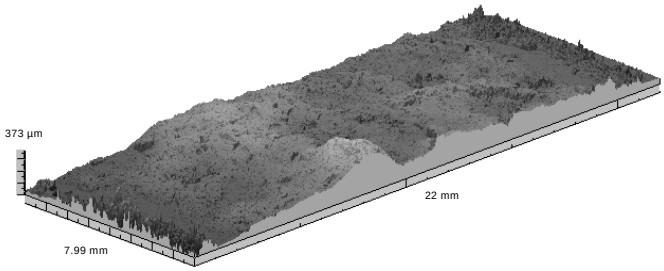

c) 8mm x 22mm section of residual coal deposit after deposit separated – peak ~350µm

Figure 5: Surface topographies of 3 different deposits from Hommel profilometer measurements.

the petcoke deposit as will be seen in the ESEM images below. This finding is particularly surprising since the petcoke ash apparent density is roughly 50% higher than that for coal ash (Table 1). One final deposition metric that is tabulated in Table 2 is the net particle capture efficiency (mg/hr of deposit divided by mg/hr of particulate in the flow). Coal has the highest capture efficiency (17%), which drops to 12% as particle loading (ppmw) is increased. The petcoke and biomass net capture efficiencies are less than half of the lowest value calculated for coal.

The coal deposit was brownish in color with a surface that was rutted and broken. The majority of the coal deposit separated from the coupon after the specimen cooled down and was removed from the holder. This left a thin (~100 µm) layer of deposit residue on the TBC. When the deposit separated from the surface, thin sheets of deposit were also dislocated from the main body of the deposit. These interface layers resembled thin sheets of mica, and later x-ray analysis indicated higher concentrations of silicon and lower concentrations of iron and aluminum relative to the bulk of the deposit. The interface sheets also registered small (~5%) but significantly elevated concentrations of potassium, phosphorus, and titanium compared to the main deposit.

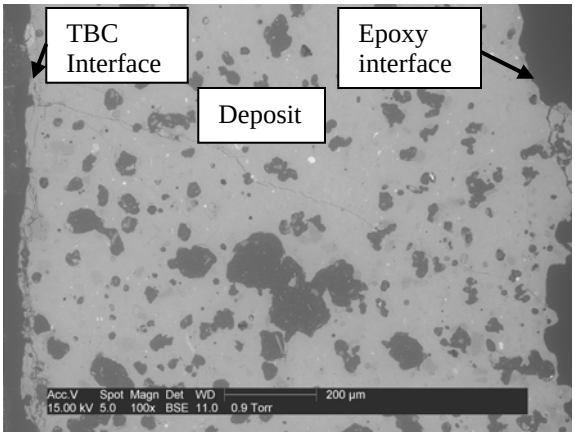

a) Coal surface deposit structure

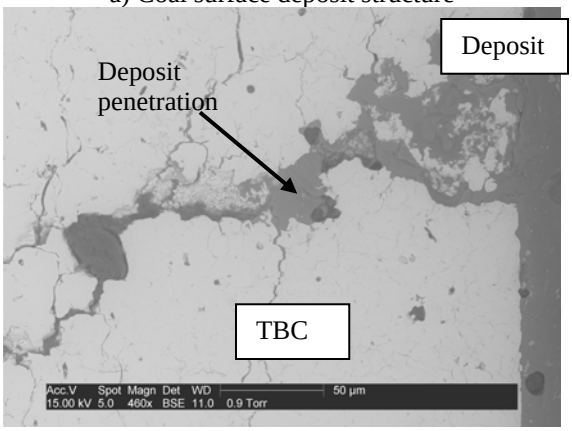

b) Coal deposit penetration into TBC

Figure 6: ESEM cross-section of coal surface deposit and coal/TBC interface.

The petcoke deposit behaved similarly to the coal deposit by separating from the coupon after test shutdown and subsequent handling. The deposit had a purplish/red color and a surface texture similar to lava rock. The dark brown sawdust deposit was considerably thinner but adhered more tenaciously than the coal or petcoke deposits. This greater adherence may be caused by its small average thickness (0.25 mm), since the residual interface stresses induced by differing coefficients of thermal expansion in the deposit and TBC decrease as the deposit becomes a thin sheet. Finally, the straw deposit had a glass-like, greenish-white surface that appeared relatively uniform in thickness. It was by far the most tenacious, with no obvious post-test dislocation from the TBC.

Surface topologies from three of the deposit samples are shown in Figure 5. The straw (5a) and coal residual (5c) surface maps represent a large fraction (8 x 22 mm) of the exposed coupon surface while the coal deposit surface map (5b) was taken from a small 3 mm x 3 mm separated piece of deposit. All three maps are shown with the surface curvature removed so that the surface roughness is highlighted. The straw deposit surface (Figure 5a) is more irregular than the coal deposit surface (Figure 5b). Centerline-averaged roughness (Ra) values are 40 µm and 28 µm for the straw and coal deposits respectively. In addition, the straw deposit roughness is steeper than the coal (average forward-facing surface angle of 23 degrees vs. 15 degrees for the coal), so the effect of the roughness on the flow is more pronounced. Comparing these

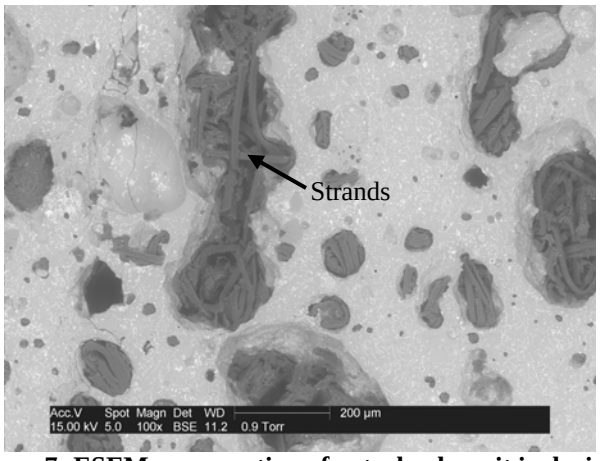

Figure 7: ESEM cross-section of petcoke deposit inclusions.

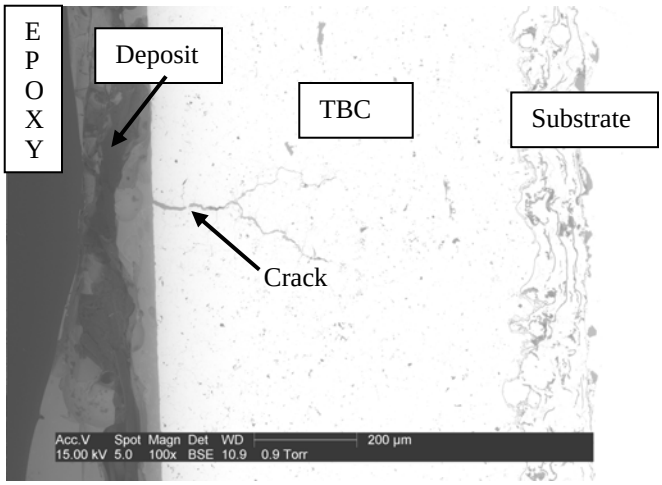

Figure 8: ESEM cross-section of straw deposit.

values to data acquired by Bons [4] for a large turbine vane operating with $Re_c \sim 1 \times 10^6$, these roughness values correspond to estimated increases in convective heat transfer coefficient ranging from 15 to 20% and increases in skin friction from 70 to 140% (for the coal and straw surfaces respectively). After the coal deposit separated from the TBC surface, the residual deposit on the specimen has a roughness signature comparable to the straw deposit (Figure 5c). Thus, if in practice large coal and petcoke deposits are removed by thermal cycling of the gas turbine, the detrimental influence on turbine efficiency due to the residual deposit could actually increase.

Scanning electron microscope (ESEM) cross-section images of the four different fuel deposits reveal significant differences in the deposit structure as well. A previous TADF study with airborne dust particles showed layering in the deposit, with structures predominantly oriented parallel to the surface [11]. By comparison, the fuel deposits in this study are fairly isotropic in structure and composition. Figure 6a is an ESEM cross-section image of the coal deposit. Note the large (±100 μm) amplitude surface height variations observed previously in the topology of Figure 5b. The coal deposit is riddled with 30-80 μm diameter inclusions. Further interrogation using x-ray spectroscopy indicated that while the majority are solid (metal) particles that were trapped in the molten deposit at temperature, some are porous cavities. The second coal ESEM image (Figure 6b) was taken at high magnification near the deposit/TBC interface. At this location, a crack in the TBC has been penetrated by the coal deposit.

The petcoke deposit (Figure 7) exhibits much larger inclusions (100-300 μm diameter) with strand-like structures lining the cavity walls. This high porosity accounts for the low density of the petcoke deposit compared to the coal deposit, as noted earlier. The isotropic matrix surrounding the inclusions registers over 60% silicon content while the strands have a composition similar to the ash. Thus the strands may be evidence of larger petcoke ash particles that were captured by the molten glass (silicon) matrix, thus greatly augmenting the deposit thickness. The sawdust deposit (not shown) exhibited a much more homogenous character with significantly fewer and smaller (10-30 μm diameter) inclusions. The straw deposit (Figure 8) is most like the airborne dust deposits mentioned earlier [11], with structures running parallel to the TBC surface.

The darkened region in Figure 8 is an elongated cavity formed during the deposition test. This deposit is the most "glass-like" and appears to have formed in sheets along the surface. A deposit-filled TBC crack is indicated in this figure as well.

While mounted in the ESEM, the deposits were interrogated using x-ray spectroscopy. The ESEM registers regions of different structure with distinctively different hues (e.g. the inclusions in Figures 6-8). Some of these regions exhibited significantly different elemental composition as well. In all cases, at least three measurements were made in each region of the deposit. The composition values in Table 3 are area-weighted averages of the various measurements. Thus, if the inclusions in Figure 6a represented 20% of the cross-sectional area of the deposit, they were averaged with a 20% weighting. Values of 0.0 indicate levels below the background noise level of the spectrometer. As has been found in previous data from actual aircraft turbine deposits [11,12], elemental concentrations showed no demonstrable trend with thickness.

Table 3: Elemental composition of deposits. (Values are in wt%).

Elements in order of atomic number	Coal	Petcoke	Straw	Sawdust
Na	5.8	3.5	4.4	5.6
Mg	4.1	1.8	2.6	7.7
Al	18.9	12.5	3.2	7.8
Si	45.3	55.0	42.6	31.8
P	1.84	0.0	6.6	0.9
S	0.9	0.0	2.0	0.9
Cl	0.0	0.0	6.7	0.0
K	2.0	1.9	15.9	4.6
Ca	11.6	6.8	7.6	34.3
Ti	1.8	1.1	3.6	0.8
V	0.0	2.2	0.0	0.0
Cr	0.0	0.3	1.2	0.0
Mn	0.0	0.0	0.0	1.8
Fe	7.8	14.5	0.0	3.8
Ni	0.0	0.5	0.0	0.0

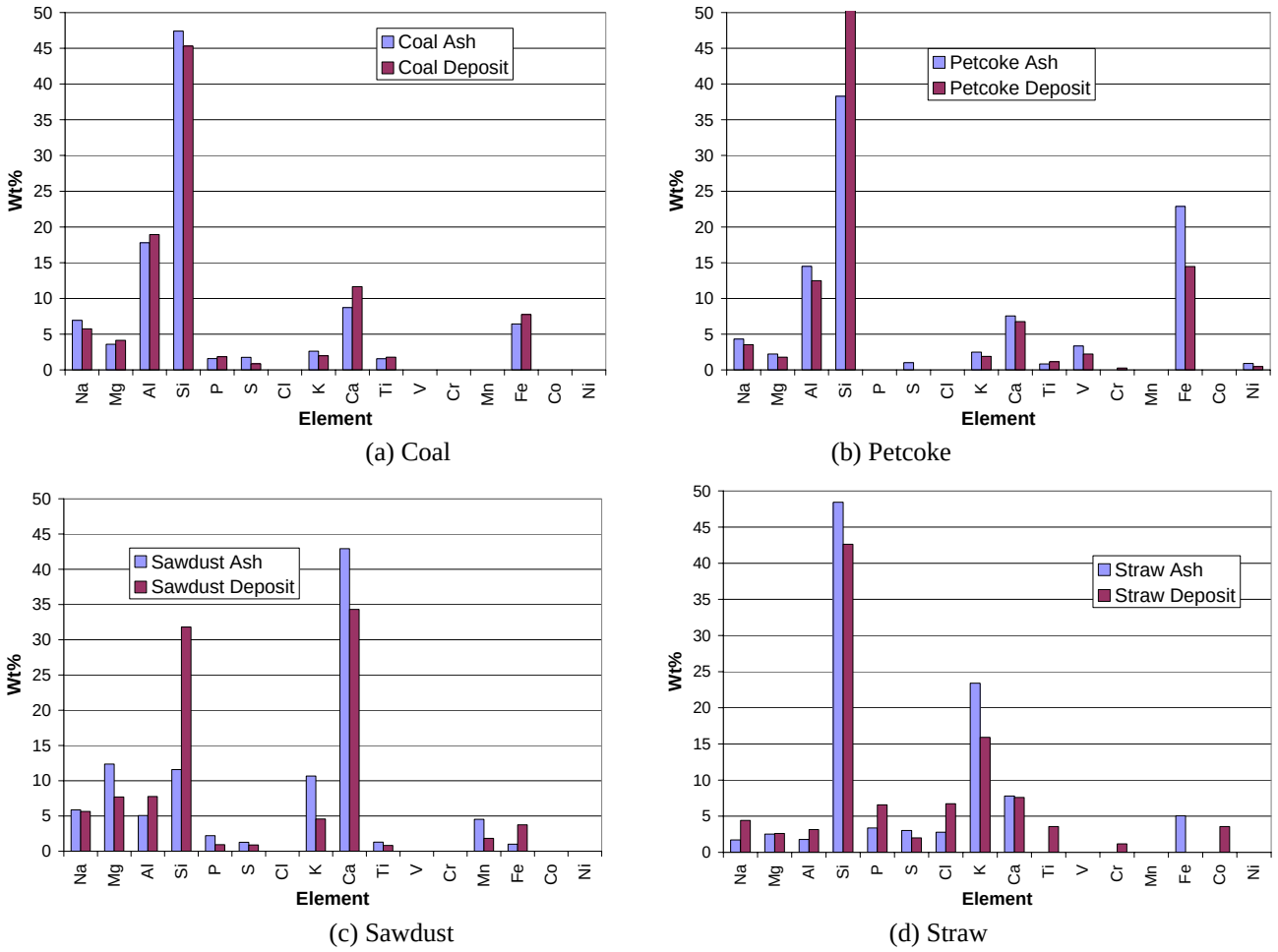

Figure 9: Comparison of element weight percent for fuel ash vs. deposit: (a) coal (b) petoke (c) sawdust (d) straw.

In general, the relative concentration of elements detected in the deposits (Table 3) are similar to those detected in the ash (Table 1). A side-by-side comparison of these data can be used to determine if there are specific preferences for deposition at the given operating conditions (Figure 9). For example, the petcoke and sawdust deposits show significant increases in the concentration of Si in the deposit (relative to the ash) at the expense of Fe (in the case of petcoke) and Ca, K, Mg (in the case of sawdust). Since silicon is non-corrosive and essentially insulates the TBC surface, this rend is favorable for blade life. On the other hand, sharp increases in Na, P, and Cl (e.g. the straw deposit) are undesirable for blade life.

Perhaps even more worrisome for the health of the turbine blade material system is the observed penetration of deposit materials into cracks in the TBC (Figures 6b and 8). These vertical segmentation cracks are deliberately formed in the air plasma sprayed (APS) TBC to improve erosion and thermal shock resistance. It is possible that these fissures present paths for premature contamination of the TBC. Though the observed deposits in the TBC cracks could possibly have been caused by contamination during specimen processing, this is considered unlikely since upon inspection with the spectrometer the penetrating deposit exhibited a unique elemental composition as compared with the surface deposits. Further study is necessary to more rigorously examine these internal deposits and determine whether this deposit penetration leads to accelerated corrosion in the base metal alloy. The deposits could also induce TBC spallation during thermal cycling due to the mismatch in coefficients of thermal expansion between the ceramic TBC and the metal deposit (similar to CMAS attack in aircraft and land-based turbines [where CMAS represents the four most common depositing oxides: calcium, magnesium, aluminum, and silicon]). Likewise, the combustion of herbaceous biomass materials, such as straws and grasses, often leads to unmanageable deposition problems in boilers. In particular, the amounts of sodium, potassium, chlorine, and sulfur in the biomass play major roles in deposition and corrosion. Potassium salts (KCl and K_2SO_4) are low melting compounds that can bind fly ash particles together and enhance the amount of deposition. There is evidence that KCl in deposits, in the absence of sulfur species, seems to initiate corrosion of superheater tubes in biomass-fired boilers [13,14,15]. The penetration of potassium and sodium into the ceramic thermal barrier coating of gas turbine surfaces is therefore important for understanding both deposition and corrosion tendencies.

CONCLUSIONS

Deposits from four alternative synfuels for the gas turbine were studied in an accelerated test facility at a gas temperature

and velocity representative of first stage high pressure turbines. Net particle loading in the accelerated testing facility is representative of operating industrial turbines though the particle size distribution was larger (mass mean diameter 10-20 μm) than typically found after proper filtration. Thus the study focuses on inertial impaction as the deposition mode. Based on the results presented in this study, the following conclusions are offered:

1) For the same net particulate loading in the gas stream, coal and petroleum coke (petcoke) produced order of magnitude larger deposits than biomass fuels. This is not proposed as a universal finding since deposition is a strong function of specific fuel type and gas temperature.
2) Though the data sample was limited, deposit thickness appears to increase linearly with particle loading for the case of petcoke and coal. Capture efficiencies ranged from 12-17% for coal to 5% and 6% for sawdust and petcoke respectively. ESEM images indicate that a molten layer of silicon on the target material may be responsible for high particle capture rates in petcoke.
3) Large (>2 mm thick) coal and petcoke deposits separate from the turbine surface following test shutdown and handling while thinner biomass deposits are more tenacious.
4) Evidence of deposit penetration into cracks in the TBC was found in all four specimens.

ACKNOWLEDGMENTS

Various individuals provided invaluable support to this research effort. The authors would particularly like to thank the assistance provided by Arun Mehta from Pacificorp for the coal flyash samples, Walt Steimel of Premcor, Harold Stocker of Cinergy, and Tampa Electric Company for assistance in locating petcoke samples, and Dr. Larry Baxter (BYU) for the biomass samples. Dr. Tom Taylor of Praxair Surface Technologies generously donated coupon specimens without which the study would not have been possible. Thanks also to Daniel Fletcher for performing particle size analysis and other helpful tasks. Michael Standing's expert assistance with the ESEM and x-ray spectrometer measurements was invaluable. Discussions with Mr. Richard Wenglarz of SCIES were helpful in establishing test matrices and framing results. This work was partially sponsored by the US Department of Energy – National Energy Technology Laboratory through a cooperative agreement with the South Carolina Institute for Energy Studies at Clemson University. The views expressed in this article are those of the authors and do not reflect the official policy or position of the Department of Energy or U.S. Government.

REFERENCES

[1] Ghenaiet, A., Elder, R. L., and Tan, S. C., "Particles and Trajectories through an Axial Fan and Performance Degradation due to Sand Ingestion," ASME Paper No. 2001-GT-497.

[2] Wenglarz, R. A., "An Approach for Evaluation of Gas Turbine Deposition", ASME Journal of Engineering for Gas Turbines and Power, vol. 114, April, 1992.

[3] Kim, J., Dunn, M.G., and Baran, A.J. et al, 1993, "Deposition of Volcanic Materials in the Hot Sections of Two Gas Turbine Engines," J. Engr. Gas Turbines & Power vol. 115, Jul 1993, pp 641-651.

[4] Bons, J. P., 2002, "St and C_f Augmentation for Real Turbine Roughness with Elevated Freestream Turbulence," Transactions of the ASME, vol. 124, OCT 2002, pgs 632-644.

[5] Wenglarz, R.A., and Fox, R.G. Jr., 1990, "Physical Aspects of Deposition From Coal-Water Fuels Under Gas Turbine Conditions", Journal of Engineering for Gas Turbines and Power, Jan 1990, pp. 9-14.

[6] Wenglarz, R.A., and Fox, R.G. Jr., 1990, "Chemical Aspects of Deposition/Corrosion From Coal-Water Fuels Under Gas Turbine Conditions", Journal of Engineering for Gas Turbines and Power, Jan 1990, pp. 1-8.

[7] Sherlock, T.P. and Wenglarz, R.A. et al., 1983, "Combustion-Turbine Design Guidelines Based on Deposition-Corrosion Considerations," Residual Fuel Oil Studies, EPRI Report AP-2739, Vol. 1.

[8] Bons, J.P., Taylor, R., McClain, S., and Rivir, R.B., "The Many Faces of Turbine Surface Roughness," *Journal of Turbomachinery*, Vol. 123, No. 4, October 2001, pp. 739-748.

[9] Patnaik, P.C., Adams, C., Fuleki, D., and Thamburaj, R., 1998, "Elevated Temperature Exposure of Gas Turbine Materials to a Bio-fuel Combustion Environment," presented at the IGTI1998, paper #98-GT-164.

[10] Wright, I.G., Leyens, C., and Pint, B.A., 2000, "An Analysis of the Potential for Deposition, Erosion, or Corrosion in Gas Turbines Fueled by the Products of Biomass Gasification or Combustion," presented at the IGTI2000, paper #2000-GT-0019.

[11] Jensen, J.W., Squire, S.W., Bons, J.P., and Fletcher, T.H., 2004, "Simulated Land-Based Turbine Deposits Generated In An Accelerated Deposition Facility," presented at IGTI 2004 in Vienna, June 2004. Paper # GT2004-53324.

[12] Borom, Marcus P., Johnson, Curtis A., and Peluso, Louis A., 1996, "Role of environmental deposits and operating surface temperature in spallation of air plasma sprayed thermal barrier coatings," Surface and Coatings Technology 86-87, pp116-126.

[13] Wall T.F., Bhattacharya S.P., Baxter L.L., Richards G., Harb J.N., "The character of ash deposits and the thermal performance of furnaces", Fuel Processing Technology, 1995, vol. 44, p. 143-153.

[14] Hein K.R.G., Heinzel T., Kicherer A., Spliethoff H., "Deposit formation during the co-combustion of coal biomass blends", Applications of Advanced Technology to Ash-Related Problems in Boilers, Edited by L.Baxter and R. DeSollar, 1996, p. 97-116.

[15] Lokare, S., Dunaway, D., Rogers, D., Anderson, M., Baxter, L., and Tree, D., "Effects of Fuel Ash Composition on Corrosion Deposits," presented at the Conference on Science in Thermal and Chemical Biomass Conversion, Victoria, British Columbia, Canada (Aug 30-Sept 2, 2004).